Marine Algae Stalk Ca^{2+} Regeneration Using Mimetic Differences

Mohsin A. Mohammed * and Miguel A. Dumett †‡

March 13, 2024

Abstract

In this study, we delve into the complex interplay of chemical reactions and diffusion processes that underpin whorl formation in marine algae, focusing specifically on the influence of external calcium concentrations. At the heart of our investigation is the application of the mimetic operators MOLE library, a sophisticated numerical tool designed for solving partial differential equations (PDEs) with high accuracy and efficiency. Through this computational lens, we elucidate the dynamic changes in marine algae whorl formation, shedding light on the critical role of calcium in mediating these processes. Our findings not only advance the understanding of marine algae's physiological responses to environmental stimuli but also demonstrate the utility of the MOLE library in tackling complex biochemical systems. This research contributes valuable insights into the reaction-diffusion mechanisms governing biological pattern formation, with potential implications for broader ecological and environmental studies

1 Introduction

Marine algae, like Acetabularia acetabulum, are fascinating single-celled organisms that can grow quite large and have complex shapes. Imagine a tiny underwater tree: it has a base that looks like roots, a long middle stalk, and a top part that fans out like an umbrella. Interestingly, this algae can also grow leaves that are about the size of a small cookie!

What's really cool about these algae is their ability to regenerate, or grow back parts that are removed. If you take off the top "umbrella," the algae can completely regrow it thanks to a special part in its base called the nucleus, where all its genetic information is stored. Even if you cut a piece from its stalk, it can grow a new top again!

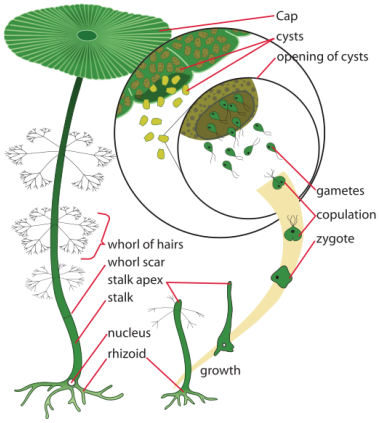

Figure 1: Algae Structure and it's body parts (taken from Wikipedia)

This study focuses on a particular aspect of the algae's growth: the formation of ring-like structures along its stalk, influenced by the amount of calcium in the water. These rings are important for understanding

*Computational Science Master's Program at San Diego State University (mmohammed5956@sdsu.edu).
†Editor: Jose E. Castillo
‡Computational Science Research Center at San Diego State University (mdumett@sdsu.edu).

how the algae grows into its unique shape, which is mainly due to chemical reactions inside the algae and its internal structure, rather than its genes. This simplified look into the algae's growth helps us learn more about how living things develop their forms in nature.

2 Related Work

Straightforward models with differential equations that excludes genetics and intracellular signaling are proposed. The pattern development is caused by the system's Turing instability as REFER(Paper) applies Murray's model, which is a purely chemical model and reaction-diffusion equation involving two reactants. In order to demonstrate the kinematic nature of this chemical diffusion model, they made the following observations: Temperature influences hair spacing, outside calcium concentration influences whorl hair spatial pattern, and whorl pattern is simultaneously initiated.

The effect of calcium concentration on the start of the whorl pattern is the main focus of this model. Whorl production requires a calcium concentration of at least 2 mM. Curiously, whorls will stop developing once more at external calcium concentrations over around 60mM. Both of these facts are demonstrated in their model, and specifics of the shift from a stable stem to whorl production when calcium concentration crosses a key value are clearly estimated. More specifically, they obtain a specific interval of calcium concentration for the whorl pattern to occur, they have shown that all three kinds of transition type can occur though in the case of thin stem wall only continuous type and catastrophic type can happen. They also show that the number of whorl hairs generated during transition can be quite irregular with underlying parameters. Besides the purpose of investigating the Acetabularia whorl formation, this paper can be viewed as an example for exploring dynamic behavior for reaction diffusion equations in an annular region.They have demonstrated that all three types of transition type can occur, even if only continuous type and catastrophic type can occur in the case of thin stem wall. More specifically, they obtain a specific interval of calcium concentration for the whorl pattern to occur. They also demonstrate how, depending on the underlying parameters, the quantity of whorl hairs produced during transition can be highly erratic. This study can be seen as an example for investigating dynamic behavior for reaction diffusion equations in an annular region, in addition to its investigation of Acetabularia whorl creation.

3 Model Equation

This is a model proposed by Murray, which is an adaptation of a simple two-species mechanism.The equations are stated as follows:

$$\begin{aligned} \frac{\partial A}{\partial t} &= D_A \Delta A + k_1 - k_2 A + k_3 A^2 B, \\ \frac{\partial B}{\partial t} &= D_B \Delta B + k_4 - k_3 A^2 B, \end{aligned}$$

where all k's and D_A, D_B are all positive parameters, A and B are functions of r, θ, and t with the annulus domain defined by

$$R_i \leq r \leq R_), \qquad 0 \leq \theta \leq 2\pi, \qquad R_i = 1,\ R_0 = 1.5.$$

A, and B define the density of two substances inside the annular growth region at the top mature Acetabularia. Here the assumption is that a reaction $2\,\mathrm{A} + \mathrm{B} \xrightarrow{\mathrm{k_3}} 3\,\mathrm{A}$ took place. Basically, B is calcium, and A could be a molecule that is increased in the calcium presence but are constantly transformed to other substances at a rate of k2. And they are generated by constant rate k1, k4 respectively for A and B.

After applying the non-dimensionalization as follows:

$$u = A\left(\frac{k_3}{k_2}\right)^{1/2},\ v = B\left(\frac{k_3}{k_2}\right)^{1/2},\ t^* = \frac{D_A t}{R_i^2},\ x^* = \frac{x}{R_i},\ d = \frac{D_B}{D_A},\ a = \frac{k_1}{k_2}\left(\frac{k_3}{k_2}\right)^{1/2},\ \lambda = \frac{k_4}{k_2}\left(\frac{k_3}{k_2}\right)^{1/2},\ R^2 = \frac{R_i^2 k_2}{D_A}.$$

Then the reaction diffusion system after omitting all the stars (*) we get the system of equations as follows

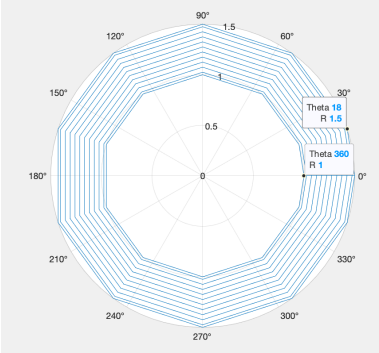

Figure 2: This is our model domain defined by R and θ in the blue color region

as follows,

$$\begin{aligned} \frac{\partial u}{\partial t} &= D\,u\,\Delta A + R^2(a - u - u^2 v) \quad \text{in } \Omega, \\ \frac{\partial v}{\partial t} &= d\,D\,v\,\Delta B + R^2(\lambda - u^2 v) \quad \text{in } \Omega, \\ u_r &= v_r = 0, \quad \text{on } \partial\Omega, \end{aligned}$$

with

$$\Delta u = \frac{\partial^2 u}{\partial r^2} + r^{-1}\frac{\partial u}{\partial r} + r^{-2}\frac{\partial^2 u}{\partial \theta^2}$$

After solving this system of equations with each other, the final PDE comes out to be in terms of u_t and v_t as follows,

$$\begin{aligned} u_t &= R^2(a - u + vu^2) + \frac{\partial^2 u}{\partial r^2} + r^{-1}\frac{\partial u}{\partial r} + r^{-2}\frac{\partial^2 u}{\partial \theta^2} \\ v_t &= R^2(b - vu^2) + d\frac{\partial^2 v}{\partial r^2} + r^{-1}\frac{\partial v}{\partial r} + r^{-2}\frac{\partial^2 v}{\partial \theta^2} \end{aligned}$$

4 Solving PDE

Mole directly calculates the Laplacian operator with single command but in our case we have to slice the Laplacian in both r and θ direction because of r^{-2}, r^{-1} terms being multiplied.

4.1 Divergence

$$\begin{aligned} D &= \nabla \cdot \mathbf{F} \\ D &= \nabla \cdot \mathbf{F} = \frac{\partial F_r}{\partial r} + \frac{\partial F_\theta}{\partial \theta} \\ D &= \begin{bmatrix} | & | \\ D_r & D_\theta \\ | & | \end{bmatrix} \end{aligned}$$

4.2 Gradient

$$\begin{aligned} G &= \nabla F(r,\theta) = \frac{\partial F}{\partial r}\hat{i} + \frac{\partial F}{\partial \theta}\hat{j} \\ G &= \begin{bmatrix} — & G_r & — \\ — & G_\theta & — \end{bmatrix} \end{aligned}$$

4.3 Laplacian

$$\begin{aligned} L &= DG \\ L &= \nabla^2 = \vec{\nabla} \cdot \vec{\nabla} \\ L &= \nabla^2 = \frac{\partial^2}{\partial r^2} + \frac{\partial^2}{\partial \theta^2} \end{aligned}$$

4.4 Initial Conditions

Bessel Functions

$$\begin{aligned} u_0 &= a + b + \epsilon(J_1(r)Y_1^{'}(1) - J_1^{'}(\delta)Y_1(\delta))\cos\theta, \\ v_0 &= \frac{b}{(a+b)^2} + \epsilon(J_1(r)Y_1^{'}(1) - J_1^{'}(\delta)Y_1(\delta))\cos\theta, \\ J_\alpha(x) &= \sum_{m=0}^{\infty} \frac{(-1)^m}{m!\,\Gamma(m+\alpha+1)} \left(\frac{x}{2}\right)^{2m+\alpha}, \\ Y_\alpha(x) &= \frac{J_\alpha(x)\cos(\alpha\pi) - J_{-\alpha}(x)}{\sin(\alpha\pi)}. \end{aligned}$$

4.5 Factorising and Boundary Conditions

$$\begin{aligned} u_t &= R^2(a - u + vu^2) + \frac{\partial^2 u}{\partial r^2} + r^{-1}\frac{\partial u}{\partial r} + r^{-2}\frac{\partial^2 u}{\partial \theta^2} \\ v_t &= R^2(b - vu^2) + d\,\frac{\partial^2 v}{\partial r^2} + r^{-1}\frac{\partial v}{\partial r} + r^{-2}\frac{\partial^2 v}{\partial \theta^2} \end{aligned}$$

Solving for u_t with implicit discretization and interpolation operators

$$\begin{aligned} u_t &= R^2(diag(a) - u + vu^2) + D_r G_r u + r^{-1} I^G G_r u + r^{-2} D_\theta G_\theta u \\ \frac{u_{new} - u_{old}}{dt} &= R^2(diag(a) - u_{new} + diag(v_{old})diag(u_{old})u_{new}) + D_r G_r u_{new} + diag(r^{-1})I^G G_r u_{new} + diag(r^{-2})D_\theta G_\theta u_{new} \\ u_{new} - u_{old} &= dtR^2 diag(a) + dt(-R^2 I + R^2 diag(v_{old})diag(u_{old}) + D_r G_r + diag(r^{-1})I^G G_r + diag(r^{-2})D_\theta G_\theta)u_{new} \end{aligned}$$

Let

$$X = -R^2 I + R^2 diag(v_{old})diag(u_{old}) + D_r G_r + diag(r^{-1})I^G G_r + diag(r^{-2})D_\theta G_\theta$$

$$\begin{aligned} u_{new} - u_{old} &= dtR^2 diag(a) + dtX u_{new} \\ (I - dtX)u_{new} &= dtR^2 diag(a) + u_{old} \\ (I - dtX + BC)u_{new} &= dtR^2 diag(a) + u_{old} \end{aligned}$$

Solving for v_t with implicit discretization and interpolation operators

$$\begin{aligned} v_t &= R^2(b - vu^2) + dD_r G_r v + r^{-1} I^G G_r v + r^{-2} D_\theta G_\theta v \\ \frac{v_{new} - v_{old}}{dt} &= R^2(diag(b) - diag(u_{new}^2))v_{new} + d\,D_r G_r v_{new} + diag(r^{-1})I^G G_r v_{new} + diag(r^{-2})D_\theta G_\theta v_{new} \\ v_{new} - v_{old} &= dt\,R^2 diag(b) + dt(-R^2 diag(u_{new}^2) + D_r G_r + diag(r^{-1})I^G G_r + diag(r^{-2})D_\theta G_\theta)v_{new} \end{aligned}$$

Let

$$Y = -R^2 diag(u_{new}^2) + D_r G_r + diag(r^{-1})I^G G_r + diag(r^{-2})D_\theta G_\theta$$

$$\begin{aligned} v_{new} - v_{old} &= dt\,R^2 diag(b) + dt\,v_{new} Y \\ (I - dtY)v_{new} &= dt\,R^2 diag(b) + v_{old} \\ (I - dtY + BC)v_{new} &= dt\,R^2 diag(b) + v_{old} \end{aligned}$$

We are using the Neumann boundary conditions. We apply the Inverse matrix in the above functions. We are using interpolation because directly applying gradient or divergence will make the points at corners but we need it to make it centre so when using MOLE we have to use Interpolation to get the points to center. After factorising and applying boundary conditions, I just ran a time loop from 0 to 2 with rate as 1e-3

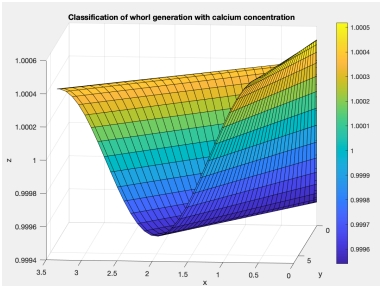

(a) Cartesian plot of U

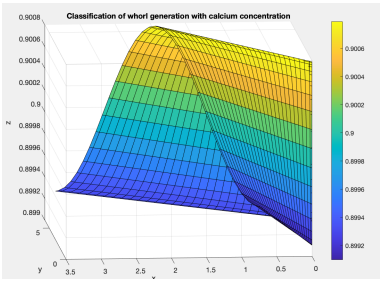

(b) Cartesian plot of V

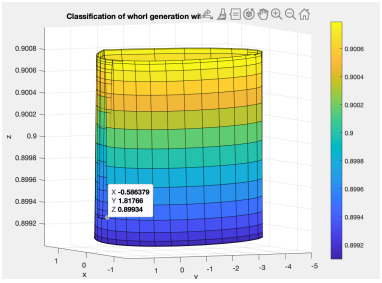

(c) Polar plot using Surf

5 Results

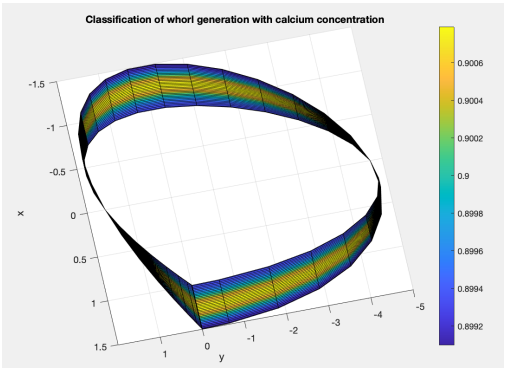

Figure 4: Polar plot using Surf, Yellow color regions depits that potentioan whorl hair growth when reaction with outside calcium concentration

6 Conclusion

In this project I solved a chemical reaction-diffusion model which is a Partial Differential Equation (PDE) using a MOLE Library. Analyzed the two reactants dynamic transitions with respect to the whorl formation of Marine algae when it is caused by outside calcium concentration on its thin annulus. More importantly, this project or chemical PDE can be good example for exploring the different dynamic behavior for reaction diffusion equations in an annular region

7 Code

```
clc
close all
clear

addpath('../mole_MATLAB')


%% Spatial discretization
k = 2;          % Order of accuracy (spatial)
m = 30;         % Number of cells in r direction
n = 30;         % Number of cells in theta direction
r1 = 1;
delta = 1.5;
```

```
r2 = delta;
theta1 = 0;
theta2 = 2*pi;
dr = (r2-r1)/m;  % Step length in r direction
dtheta = (theta2-theta1)/n; % Step length in theta direction


%% 2D Staggered grid
r_grid = [r1 r1+dr/2 : dr : r2-dr/2 r2];
theta_grid = [theta1 theta1+dtheta/2 : dtheta : theta2-dtheta/2 theta2];

[r_pts, theta_pts] = meshgrid(r_grid, theta_grid);
x = r_pts.*cos(theta_pts);
y = theta_pts.*sin(theta_pts);

[x1, y1] = pol2cart(r_pts, theta_pts);


%% Parameters
a = 0.1;
b = 0.9;
d = 9;
R = 3.45;
epsilon = 1e-2;

%% Simulation time
t_end = 0.5;
dt = 0.01;

%% Bessel functions calculation
Jn = besselj(1, r_grid);
Yn = besselj(2, r_grid);
J1 = besselj(1, r_pts);
Y1 = Yn(end);
DJn = diff(Jn) / dr;
DYn = diff(Yn) / dr;
DJ_delta = DJn(end);
DY1 = DYn(1);

%% IC
U0 = a + b + epsilon*((J1*DY1)-(DJ_delta*DY1)).*cos(theta_grid);
V0 = (b/(a+b)^2) + epsilon*((J1*DY1)-(DJ_delta*DY1)).*cos(theta_grid);

U_old = U0(:);
V_old = V0(:);

%% Equation discretization
D = div2D(k, m, dr, n, dtheta);
G = grad2D(k, m, dr, n, dtheta);

Dr = D(:,1:n*(m+1));
D_theta = D(:,n*(m+1)+1:end);

Gr = G(1:n*(m+1), :);
G_theta = G(n*(m+1)+1: end, :);
```

```
69
70  r_pts = r_pts(:);
71  theta_pts = theta_pts(:);
72
73  IG = interpGMat2D(k, m, n);
74  I_Gr = IG(:,1:n*(m+1));
75
76  %% BC
77  BC_term_eq = robinBC2D(k, m, dr, n, dtheta, 0, 1);
78
79  %% Time loop
80  for t = 0 : dt : t_end
81      X = R^2 * diag(V_old) * diag(U_old)                ...
82          + (Dr * Gr) + (diag(1./r_pts) * I_Gr * Gr)  ...
83          + (diag(1./r_pts.^2) * D_theta * G_theta)   ...
84          - R^2*diag(length(U_old));
85      X = eye(length(U_old), length(U_old)) - dt*X + BC_term_eq;
86      U_new = inv(X)*(dt*R^2*a*ones(length(U_old),1))+U_old;
87
88
89      Y = (d*(Dr*Gr) + diag(1./r_pts) * I_Gr * Gr)  ...
90          + (diag(1./r_pts.^2) * D_theta * G_theta)  ...
91          - R^2* diag(U_new) * diag(U_old);
92      Y = eye(length(V_old), length(V_old)) - dt * Y + BC_term_eq;
93      V_new = inv(Y)*(dt*R^2*b*ones(length(V_old),1)+V_old);
94
95      U_old = U_new;
96      V_old = V_new;
97
98      subplot(2,2,1);
99      surf(x1,y1,reshape(U_new, m+2, n+2));
100 % %
101     subplot(2,2,2);
102     surf(x1,y1,reshape(V_new, m+2, n+2));
103
104     subplot(2,2,3);
105     surf(x,y,reshape(U_new, m+2, n+2));
106     subplot(2,2,4);
107     surf(x,y,reshape(V_new, m+2, n+2));
108
109 %     title('Classification of whorl generation with calcium concentration');
110     xlabel('x')
111     ylabel('y')
112     zlabel('z')
113
114     colorbar
115     drawnow
116
117
118 end
```

References

[1] Corbino, J., and Castillo, J.E. High-order mimetic finite-difference operators satisfying the extended Gauss divergence theorem. In: Journal of Computational and Applied Mathemat-

ics 364 (2020), p. 112326. issn: 0377-0427. doi: https://doi.org/10.1016/j.cam.2019.06.042. url: https://www.sciencedirect.com/science/article/pii/S0377042719303231.8\item command.

[2] Mao, Y., Yan, D., and Lu, C.H., Dynamic transitions and stability for the acetabularia whorl formation. arXiv:1810.10120 [math.AP]

[3] Murray, J.D., Mathematical biology II: Spatial models and biomedical applications, 3rd edition, Springer-Verlag, New York, 2001.

[4] Ma, T., and Wang, S., Bifurcation theory and applications, vol. 53, World Scientific, 2005.

[5] Ma, T., and Wang, S., Phase transition dynamics, Springer, 2014.

[6] Martynov, L., A morphogenetic mechanism involving instability of initial forth, Journal of theoretical biology, 52 (1975), 471–480.